

3.6.3

Development of position-sensitive scintillation neutron detectors at J-PARC/MLF

Tatsuya Nakamura¹, Kentaro Toh¹, Kaoru Sakasai¹, Katsunori Honda¹, Kazuhiko Soyama¹, Masaki Katagiri²

¹J-PARC Center, JAEA, Tokai, Ibaraki 319-1195, Japan

²Frontier Research Center for Applied Atomic Sciences, Ibaraki University, Tokai, Ibaraki 319-1195, Japan

E-mail: nakamura.tatsuya@jaea.go.jp

Abstract. Development of position-sensitive scintillator detectors at the J-PARC/MLF is briefly reviewed. This paper focuses on the detectors particularly using wavelength shifting fiber technology. Recent R&D works including a time-of-flight neutron imager and those for alternative to helium-3 gas detectors are also presented.

1. Introduction

Position-sensitive neutron detectors have been intensively developed for neutron scattering instruments for decades. Particularly those detectors with scintillation technology have been acknowledged indispensable for pulsed neutron diffraction instruments. Many of superior position-sensitive scintillation detectors have been developed at ISIS detector group. They have carefully tailored and optimized the detector performances depending on the purposes, providing the state-of-the-art detectors to their neutron instruments [1].

The development of position-sensitive scintillator detectors for J-PARC was initiated in the late '90s. An emerging WLS fiber technology seemed suitable at the time to design for detectors with various characteristics adjusted to the neutron scattering instruments in the MLF of the J-PARC. Although it had not yet convinced whether a WLS fiber technology could meet a high requirement in terms of gamma-ray insensitivity Dr. Katagiri took a decisive step to challenge in developing scintillator detectors using wavelength-shifting (WLS) fibers.

In this paper we briefly review the two-dimensional detectors developed using WLS fibers for neutron scattering instruments, iBIX and SENJU, in the J-PARC/MLF. In addition we introduce a progress in scintillator phosphor development. Finally recent works including the time-of-flight neutron imager and the detector for alternative to helium-3 gas detectors are presented.

2. Wavelength-shifting fiber based scintillation detector

2.1. iBIX detector

The iBIX is a single crystal diffractometer for biomolecular crystallographic study. The two-dimensional detector for iBIX (called iBIX detector, hereafter) was our first WLS-fiber-based scintillation detector developed in the J-PARC/MLF. The specifications required to the detector were quite challenge at the time. Bragg peak intensities on the detector in the instrument had been expected very low hence the detector had to have a high detection efficiency, more than 50% for thermal

neutrons whilst maintaining acceptable gamma-ray sensitivity to the order of 10^{-6} . The detector also had to be designed compact with modularity to enable multiple detectors tiled around the sample. Each detector should have the least neutron-insensitive area over the detector face to increase packing rate. Moreover a severe peak separation in space demanded a detector to have a spatial resolution of less than 1 mm. No such detector had been ever commercially available except paying unacceptably low detector efficiency.

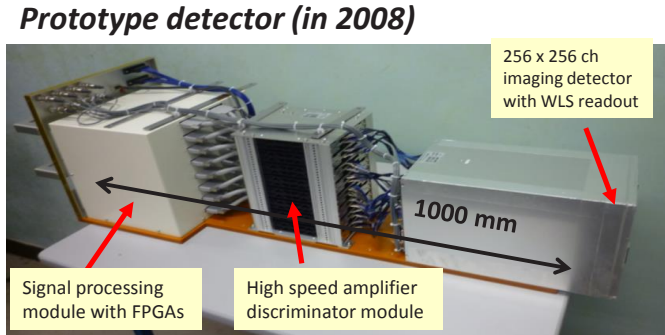


Figure 1. A prototype detector for iBIX instrument.

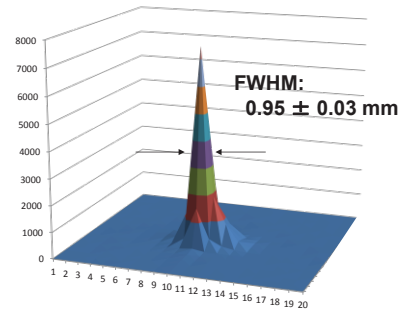


Figure 2. A collimated beam measured with the iBIX detector.

The WLS fibre technology has been intensively used in high energy physics experiments. There for gamma-ray or x-ray detection a single scintillator screen is usually sandwiched with WLS fibre ribbons from the top and bottom in favour of light collection. In order to make it suitable to neutron detection new detector head structure was introduced, where two ^{10}B -doped ZnS scintillator screens actually sandwich the crossed WLS fibres arrays [2]. By doing so a number of the scintillator screens became double ensuring a high neutron capture rate, thus for detection efficiency.

Figure 1 shows a prototype detector produced in 2008. The physical size is almost identical to the one installed in the iBIX. The detector has a neutron-sensitive area of $133 \times 133 \text{ mm}^2$, making a filling factor to 69% over the detector face [3]. Each WLS fiber connects one of the pixels in a multi-anode PMT. Detector electronics: 256×2 channels of amplifier and discriminator cards and the signal processing module, are placed behind the detector head so that to make the detector compact and modular. The detector operates in a photon counting method.

The detector head is made with packed 1/2-mm diameter WLS fibre ribbons. This makes the detector pixel size small enough to measure precise structure of Bragg peaks. Figure 2 shows a measured beam profile when a neutron beam was collimated with 1-mm diameter incident to the detector. The detector measured the collimated beam $0.95 \pm 0.03 \text{ mm}$ in full width at half maximum, reproduced the beam profile very well. This result indicated that the detector has a spatial resolution less than 1 mm and it is close to the pixel size of 0.5 mm. The achieved spatial resolution is nearly approaching to the “light spread limit”, which is calculated including light scattering within the scintillator and the fibre arrays [4].

2.2. SENJU detector

We have developed a two-dimensional detector that has larger area than the iBIX detector for SENJU in the J-PARC [5]. The SENJU is also a single crystal diffractometer that sees one of the poisoned moderators in the J-PARC/MLF. The SENJU required a large area and a large number of detector modules for scanning a wide range of reciprocal space in one measurement. The major differences from the iBIX detector are: a large neutron-detective area with a moderate spatial resolution, a count rate capability up to 50 kcps, and a tolerance to leakage magnetic field up to 200G. Figure 3 shows a schematic view of the neutron-detecting head. We have made following changes in the detector head:

add the air gap deliberately between the WLS fibres instead of packing to each other, spliced the WLS fiber to the clear fiber which is bent backward with a radius of 3 mm to minimize the dead area.

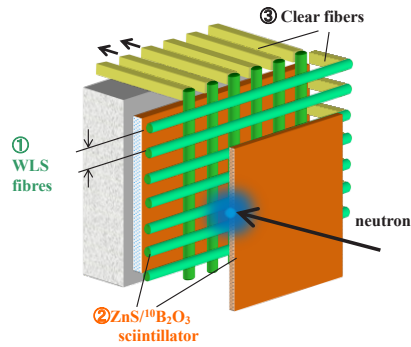
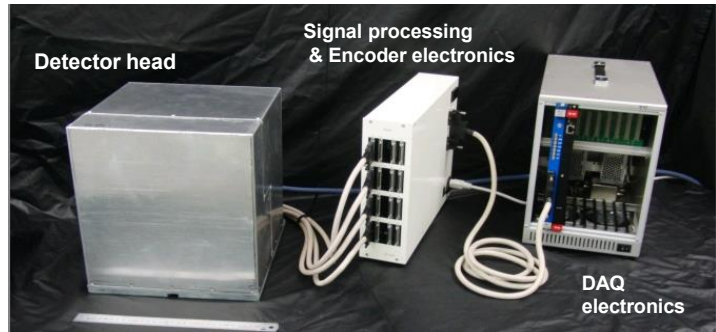


Figure 3. A schematic view of detecting head of SENJU detector.



T. Nakamura, et al. NIM -A, 686(2012)64.

Figure 4. Detector system of SENJU [5].

The dual scintillator screens are maintained similar to the iBIX detector. With this design the detector becomes to have a large coverage at an affordable cost, high detection efficiency and minimized neutron-insensitive area.

Figure 4 shows detector system of SENJU (showing only one detector module). The detector module is designed to have a neutron-sensitive area of $256 \times 256 \text{ mm}^2$ with a 4-mm spatial resolution. One signal processing & encoder electronics can handle four detector modules, which saves a lot with detector electronics. The neutron event data are recorded in list mode for post data processing.

2.3. R&D for Scintillator phosphor

We have developed the new ZnS phosphor intensively to decrease its afterglow to ensure a count rate capability of the detector. With the commercial ZnS scintillator the afterglow lasts for a few tens of

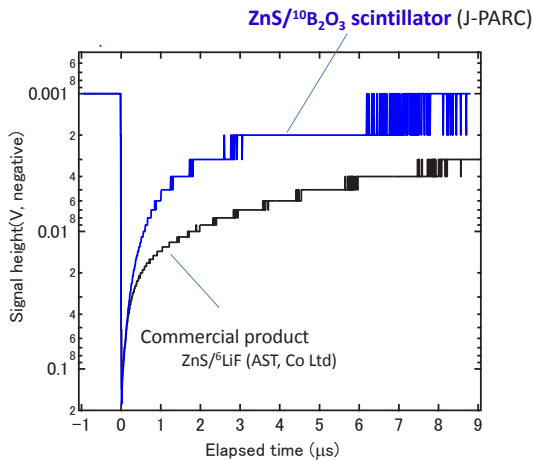


Figure 5. Comparison of the averaged waveforms of neutron-induced signals [6].

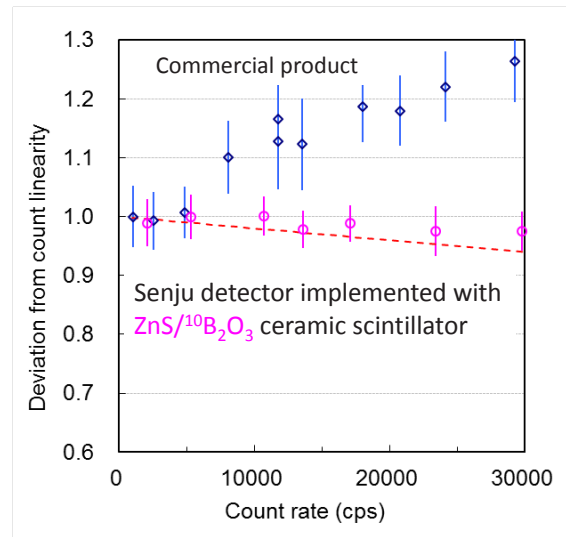


Figure 6. Normalized count rate of the SENJU detector implemented with a commercial product ($\text{ZnS}/^6\text{LiF}$) and the developed scintillator ($\text{ZnS}/^{10}\text{B}_2\text{O}_3$) [6].

microseconds, which kills a count rate capability of the detector significantly with our signal processing method.

Figure 5 shows averaged neutron-induced signal waveforms of the commercial products ($\text{ZnS}/^6\text{LiF}$ produced by AST Co. Ltd) and our scintillator made with new ZnS phosphor ($\text{ZnS}/^{10}\text{B}_2\text{O}_3$) [6]. The both signals had similar primary decay time constant of ~ 60 ns, but our scintillator exhibited much lower afterglow than the commercial product (The afterglow decreased about one thirds compared to the commercial product.) Note that the averaged signal exhibited similar pulse height at the beginning part, indicating that the new scintillator would not decrease detector efficiency much with a proper signal processing although a total amount of detected photons became less compared to the commercial product.

Figure 6 shows the normalized count rates of the SENJU detector implemented with the commercial scintillator and the new $\text{ZnS}/^{10}\text{B}_2\text{O}_3$ scintillator screen. The count rate of the detector was divided by the count measured by a detector monitoring the incident neutrons (a ^3He detector with a detection efficiency of $\sim 10^{-4}$ for thermal neutrons), with the resultant normalized ratio facilitating comparisons with the theoretical calculations. With the commercial scintillator the detector suffered a lot with multicounting at more than count rate of 5kcps, resulting in the significant deviation from the theory. It was clearly shown that the count rate follows nearly to the theoretical calculation up to 30 kcps with the new scintillator, extending our count rate capability by a factor six compared to the one with the commercial product.

2.4. Detectors installed in the beam lines

Figure 7 shows the photograph of the detectors in the iBIX. 30 detector modules have been installed in the detector banks by the end of 2013. Figure 8 shows a view of the SENJU at present. The detector banks have fully populated with the detector modules by the end of 2013. Total 37 detectors cover 30% of the solid angles around the sample [7].

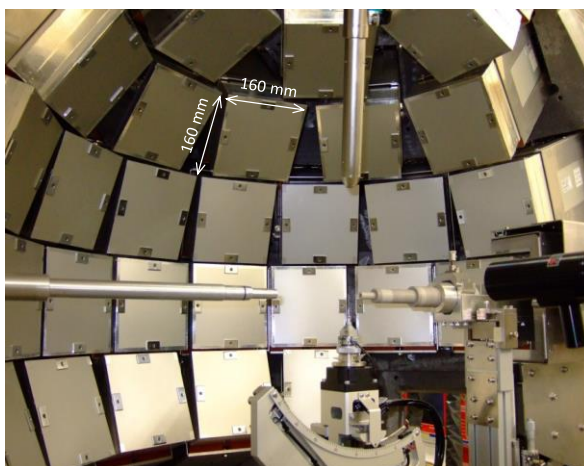


Figure 7. Photograph of the iBIX.



Figure 8. Photograph of the SENJU.

3. Time-of-flight neutron imager with WLS fiber technology

Apart from beam line detectors we have been working detector R&D that could be useful or may have some possibilities for future neutron scattering instruments. Development of a time-of-flight neutron imager is one of such activities. It has been acknowledged that neutron radiography or neutron tomography is a powerful non-destructive technique to visualize an object what is not seen with other radiations such as by x-rays. We tried to see a possibility of making such detector using WLS fibre technology. Particularly the detector that can meet the requirements both in a spatial resolution less

than 100 μm and low gamma-ray sensitivity is a challenge over the conventional detectors such as CCD, MSGD, ^6Li -loaded glass scintillator. So far neutron-sensitive micro-channel plate detector offers promising prospects in terms of a spatial resolution and count rate but it is hard to have a capability of rejecting gamma-ray to the level of 10^{-7} in principle.

Figure 9 shows a schematic view of a detector head of the proposed neutron time-of-flight imager [8]. The detector is comprised of a thin scintillator screen, a light image magnifier made of a fiber optic taper, and WLS fiber arrays. The idea is that the magnified neutron(light) image by a factor of 3.1 is measured with the light sensors with a fine pixel size. For this purpose the dedicated WLS fibers with a diameter of 100 μm were produced, which is the smallest ever made as a WLS fibre as far as we acknowledge. In combination with the proper image magnifier the effective size of the detector pixel becomes $34 \times 34 \mu\text{m}^2$.

Figure 10 shows a measured beam profile covered with a Cd mask on the detector face. The detector exhibited a spatial resolution of 68 μm in FWHM, which is the best achieved ever with this type of detector. The detector also exhibited a gamma-ray sensitivity of less than 10^{-7} thanks to the thin thickness of the ZnS screen and the less amounts of WLS fibers.

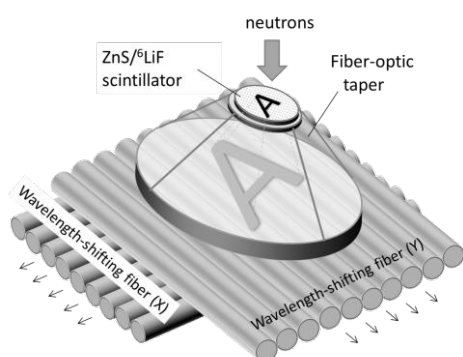


Figure 9. A schematic view of the WLS fiber detector with a sub 100- μm spatial resolution [8].

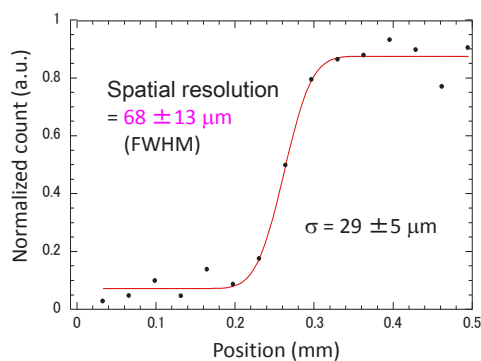


Figure 10. Fitting result to beam edge profile measured with Cd mask on the detector face [8].

4. Detectors as alternative to helium-3 gas based PSDs

Recent world-wide shortage of ^3He gas has accelerated the development of neutron detector technologies that could be alternative to conventional ^3He -gas-based detectors. We have been working on the scintillation neutron detectors that could be used for inelastic neutron scattering instruments in

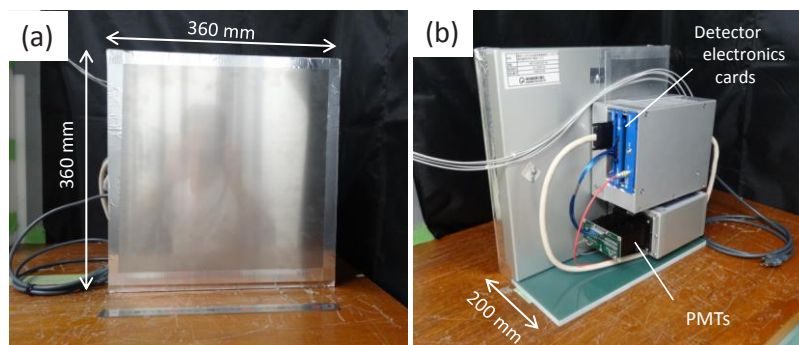


Figure 11. Photograph showing (a) front and (b) rear view of the prototype detector [9].

future under the frame work of international collaboration on neutron detectors. Two lines of development works are underway at the J-PARC/MLF. One is a SENJU type detector which is aimed at installing outside of a vacuum tank and the other is the scintillator WLS fibre coil detector called SFC detector which is aimed at installing inside a vacuum tank.

4.1. SENJU type detector

The SENJU type detector follows almost similar to the detector structure with the SENJU detector. A pitch of the WLS fibres is 5 mm, in contrast to 4 mm in the original detector, which increases the neutron-sensitive area of the detector by a factor of 1.56. The pixel size can be made larger (i.e. $20 \times 20 \text{ mm}^2$) to decrease a number of electronics while keeping the size of detector pixel small enough for inelastic neutron scattering instruments. This can be done by reading out four WLS fibres as potting into one PMT channel which ensures reasonable light-collection efficiency with great flexibility in pixel size. Figure 11 shows a photograph of the prototype detector. The detector is designed to have a neutron-sensitive area of $320 \times 320 \text{ mm}^2$. The detector is designed to be compact and light weighted with a physical size of $360 \times 360 \times 200 \text{ mm}^3$. The weight of the detector is 11.6 kg. All of the detector electronics—including PMTs, the amplifier/discriminator card, the high-voltage card and the signal processing/encoder card—are made dedicated for this detector and installed behind the neutron-detecting head.

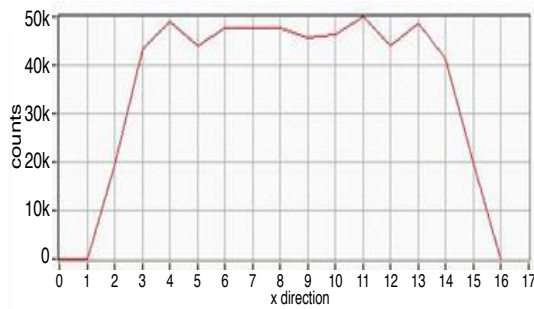


Figure 12. Count projection measured with a prototype detector.

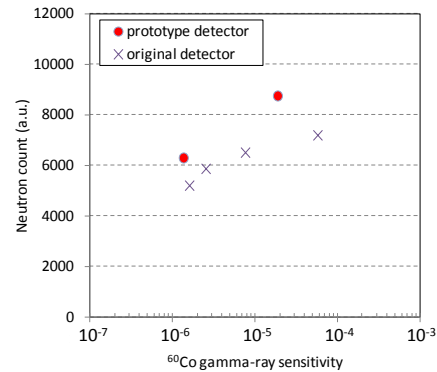


Figure 13. Neutron count versus ^{60}Co gamma-ray sensitivity [9].

Figure 12 shows count projection along x-direction. The count uniformity was evaluated as about 15% (SD) by Gaussian fitting, which would be acceptable for most neutron-scattering experiments (the scintillator screens that have a size of $256 \times 256 \text{ mm}^2$ are temporarily implemented at present). Figure 13 shows the detector metrics, with the neutron count (detection efficiency) plotted versus the ^{60}Co gamma-ray sensitivity. The data measured with the original detector are included for comparison. At the ^{60}Co gamma-ray sensitivity of 10^{-6} (the normal operating condition), the prototype detector exhibited 20% larger neutron counts than the original detector, with a calibrated detection efficiency of about 40% for thermal neutrons. Increasing the area of the detector would be the future task together with lowering the intrinsic background rate.

4.2. Scintillator WLS fiber coil detector

The idea of the scintillator WLS fiber coil detector is to make the detector element with a rolled WLS fibre coil sandwiched with the rolled cylindrical scintillator screens[10]. With these elements the detector can be made tubular shape and long that would make it much easy to be installed in the vacuum tank. Since the incidence neutron experiences four layers of scintillation screens the detector has a potential to have high detection efficiency, which is similar to that of the 6-bar 1-inch diameter

^3He gas PSD. Moreover the detector is pixelated, so the detector can operate at much higher global count rate per tube than the conventional ^3He gas PSD.

Figure 14 shows the demonstrator detector that has 64-elements and a 1-inch diameter ^3He gas-based PSD for comparison. The element size of the SFC detector is made 22×20 mm to fit in the 1-inch diameter Aluminium tube (although the present diameter of the demonstrator detector tube is 30 mm due to a ready availability). Clear fibres from each coil elements penetrate through the tube centre to the multianode-PMTs which are placed at one end of the tube. At present the detector exhibited detection efficiency of 35-45% for thermal neutrons with an acceptable gamma sensitivity and multicount rate. This can be improved by optimizing the fiber coil structure and minimizing the light loss at the splicing parts between the WLS and clear fiber.

Figure 15 shows normalized beam profiles with a Cd mask measured using the ^{252}Cf source. A cylindrical piece of rolled Cd with a thickness of 0.7 mm and a length of 225 mm covered the left, centre and right areas of the detector. The detector reproduced the profile of the masked beam very well: the detector measured the masked area as ~ 220 mm (10.5 pixels) at full width at half maximum for all the masked positions, demonstrating the capability of the one-dimensional position sensitivity of the detector.

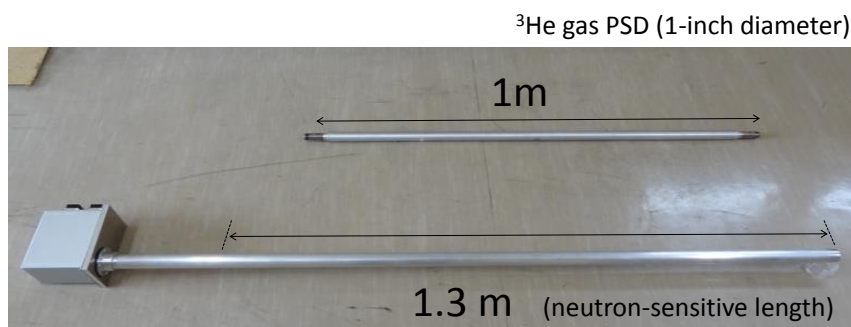


Figure 14. Photograph of a 64-element SFC detector (1-inch diameter ^3He gas PSD is also shown as reference) [10].

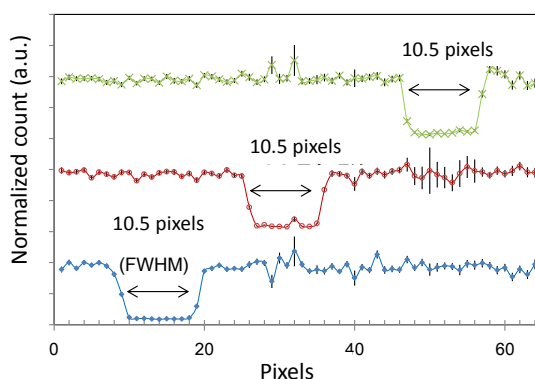


Figure 15. Normalized beam profiles with a Cd mask measured using the ^{252}Cf source [10].

5. Summary

We have intensively developed position-sensitive scintillation neutron detectors by using WLS fiber technology. The WLS fiber technologies add great flexibility to detector designs and the detector

structure has been optimized for iBIX and SENJU. New scintillator material that can improve a count rate capability of the detector has been developed and its feasibility demonstrated. Further detector development for alternative to ^3He gas PSDs will continue for future.

6. References

- [1] ISIS facility: <http://www.isis.stfc.ac.uk/>
- [2] Katagiri M, et al. 2004 *Nucl. Instr. & Meth. A* **529** 313
- [3] Hosoya T, et al. 2009 *Nucl. Instr. & Meth. A* **600** 217
- [4] Nakamura T, et al. 2014 *J. of Instr.* **Vol 9** C11020
- [5] Nakamura T, et al. 2012 *Nucl. Instr. & Meth. A* **686** 64
- [6] Nakamura T, et al. 2014 *J. of Phys. Conf. ser.* **528** 012043
- [7] Kawasaki T, et al. 2014 *Nucl. Instr. & Meth. A* **735** 444
- [8] Nakamura T, et al. 2014 *Nucl. Instr. & Meth. A* **737** 176
- [9] Nakamura T, et al. 2014 *J. of Phys. Conf. ser.* **528** 012042
- [10] Nakamura T, et al. 2014 *Nucl. Instr. & Meth. A* **741** 42